ORIGINAL RESEARCH

Check for updates

Different reactivity to glutathione but similar tumor cell toxicity of chalcones and their quinolinone analogues

Giulio D. C. d'Oliveira[1,2] · Jean M. F. Custodio[1] · Andrea F. Moura[3] · Hamilton B. Napolitano[4] · Caridad N. Pérez[1] ·
Manoel O. Moraes[3] · László Prókai[5] · Pál Perjési [6][2]

Abstract

Non-enzyme catalyzed nucleophilic addition of reduced glutathione (GSH) onto two open-chain sulfonamide chalcones and two quinolinone-chalcone hybrids were studied to investigate the relationship between tumor cell cytotoxic activities and GSH-reactivities of the compounds. The consumption of the chalcones or the quinolinone-chalcone hybrids due to conjugation with GSH was evaluated by analytical high-performance liquid chromatography, and the formed diastereomeric adducts were identified by liquid chromatography–mass spectrometry. When the reaction was conducted with the open-chain chalcones, the equilibria were shifted towards formation of the respective GSH-conjugates. On the other hand, the cyclic chalcone derivatives with the quinolinone moiety were found to equilibrate to mixtures containing predominantly the reactants despite the strong electron withdrawing group present in the B-ring of the compounds. The observed opposite behavior can be rationalized by reduced thiol-reactivity of the quinolinone-chalcone hybrids and fast decomposition of their GSH-conjugates. A combined X-ray diffraction and theoretical approach were used to explain the observed difference in the reactivities towards GSH. However, structural differences did not influence tumor cell (SF-295, PC-3 and HCT-116) cytotoxicity of the evaluated compounds. Accordingly, the altered GSH-reactivity seems to be not a determining factor in the tested tumor cell cytotoxic activity of the investigated compounds.

Keywords Chalcones · Quinolinone · Glutathione · Michael reaction · Tumor cell cytotoxicity.

✉ Pál Perjési
pal.perjesi@gytk.pte.hu
pal.perjesi@gmail.com

[1] Instituto de Química, Universidade Federal de Goiás,
Goiânia, Goiás 74690-900, Brazil

[2] Institute of Pharmaceutical Chemistry, University of Pécs, Pécs
H-7624, Hungary

[3] Núcleo de Pesquisas e Desenvolvimento de Medicamentos,
Universidade Federal do Ceará, 60430-270 Fortaleza, Ceará,
Brazil

[4] Ciências Exatas e Tecnológicas, Universidade Estadual de Goiás,
Anápolis, Goiás 75132-903, Brazil

[5] Department of Pharmacology and Neuroscience, Institute of
Healthy Aging, Graduate School of Biomedical Sciences,
University of North Texas Health Science Center, Fort Worth,
Texas 76107, USA

Introduction

Chalcones are intermediary compounds of biosynthetic pathways of a very large and diverse group of plant constituents known collectively as flavonoids (Harborne and Williams 2000). Among the naturally occurring chalcones and their synthetic analogs, several compounds displayed cytotoxic (cell-growth inhibiting) activity towards cultured tumor cells. Chalcones also are effective in vivo as cell-proliferation inhibitors, anti-tumor promoting, anti-inflammatory and chemopreventive agents (Go et al. 2005; Nowakowska 2007; Amslinger 2010; Rahman 2011; Sahu et al. 2012; Maydt et al. 2013; Sing et al. 2014; Rozmer and Perjési 2016; Gomes et al. 2017; Zhuang et al. 2017).

Nucleophilic addition of cellular thiols onto the polarized carbon-carbon double bond (Michael-reaction) is frequently associated with the biologic effects of chalcones and other α,β-unsaturated carbonyl compounds (Go et al. 2005; Nowakowska 2007; Amslinger 2010; Maydt et al. 2013; Gomes et al. 2017; Perjési et al. 2019). Such a reaction

involving reduced glutathione (GSH) can alter intracellular redox status (redox signaling), which can modulate events such as DNA synthesis, enzyme activation, selective gene expression, and regulation of the cell cycle Modification of cellular redox status through GSH-conjugation could result in both desired and undesired (e.g., cancer resistance) effects of the compounds (Powis et al. 1997; Estrela et al. 2006; Ortega et al. 2011; Traverso et al. 2013; Harris et al 2015; Bansal and Simon 2018; Vasková 2019).

Several biological effects (e.g., NQO1-inducer (Dinkova-Kostova et al. 2001), anti-inflammatory (Jin et al. 2008; Amslinger 2010; Maydt et al. 2013;), GST P1-1 inhibitory (Wang et al. 2009) of chalcones have been associated with their Michael-type reactivity towards GSH. It was suggested that the lower anti-inflammatory potential of chalcones with strong electron donor substituents (e.g., dimethylamino) on the B-ring could be the consequence of the lower Michael-type reactivity of the derivatives towards GSH (Jin et al. 2008). On the other hand, higher reactivity towards GSH and other thiols were found to parallel with higher NQO1-inducing potential of the investigated chalcones (Dinkova-Kostova et al. 2001). The results highlighted importance of the GSH-conjugation of chalcones, which can be an important molecular event in the mechanism of their biological actions.

Structural modification of chalcones could result in different GSH-reactivity (Amslinger 2010; Maydt et al. 2013; Gomes et al. 2017). Earlier, we have investigated GSH-reactivity of analogous 4′-hydroxychalcones and their bis-Mannich derivatives (Bernardes et al. 2017; Bernardes et al. 2018). It was found that the Mannich derivatives showed a significantly different reactivity (Bernardes et al. 2017) and stereoselectivity (Bernardes et al. 2018) from those of the respective non-Mannich derivatives when the reactions were conducted under acid conditions. Furthermore; we have synthesized several 2′-benzensulfonamido-chalcones and their cyclic quinolone derivatives (de Castro et al. 2016; de Castro et al. 2017; d'Oliveira et al. 2018). Some of the chalcones showed excellent inhibition of cell growth of HCT-116 (colon) tumor cells. On the contrary, only a small fraction of the cyclic analogues displayed comparable inhibitory activity (d'Oliveira et al. 2018).

In order to investigate how the conversion of the open-chain 2′-sulfonamide chalcones to the respective quinolone derivatives affect the cytotoxicity and the GSH-reactivity, here we report on the GSH addition and tumor cytotoxic determination of two sulfonamide chalcones (2 and 3) and their cyclic quinolinone analogs (5 and 6) (Fig. 1). Compounds 5 and 6 have the same chalcone moieties as compounds 2 and 3, which allow comparison of GSH-reactivity towards the enone derivatives regarding this particular change in structure (i.e., open-chain *versus* cyclic quinolinone). For a better understanding of the observed
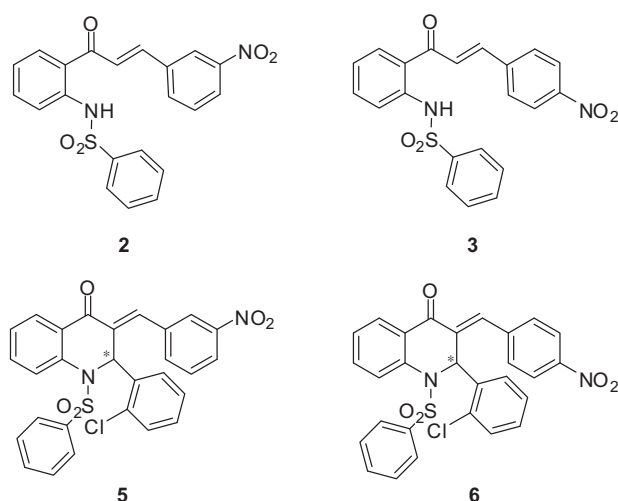
Fig. 1 Structural formula of chalcones **2** and **3** and quinolinones **5** and **6**

differences in reactivity, the crystal structure of chalcones **2** and **5** was determined by X-ray diffraction, and theoretical calculations were performed. Cytotoxicity of the compounds was evaluated against the SF-295 (glioblastoma), PC-3 (prostate cancer) and the HCT-116 (colon cancer) tumor cell lines and the results were compared with the observed GSH-reactivities.

Materials and methods

Synthesis

General Information

Compounds **1**, **2**, **4**, **5** and **6** were synthesized as published before (d'Oliveira et al. 2018). Characterization of the synthesized samples were accomplished by their melting points, and their ^1H ^{13}C NMR, and HRMS spectra. The respective ^1H ^{13}C NMR spectra (Figures S1-S6), ^{13}C NMR spectra (Figures S7-S12), and HRMS spectra (Figures S13-S18) of the compounds can be found in the Supplementary Data.

Melting points were determined with the solid supported on glass coverslips using a Karl Kolb (Frankfurt, Germany) apparatus. NMR spectra were acquired on a Bruker (Bremen, Germany) Avance III 500 spectrometer operating at 11.75T, observing ^1H at 500.13 MHz for the hydrogen nucleus or 125.76 MHz for the carbon nucleus. The complete signal assignment was also obtained by heteronuclear multiple bond correlation (HMBC) and heteronuclear single quantum correlation (HSQC) experiments. Mass spectrometric analysis was performed using a Micro-TOF-Q III spectrometer (Bruker Daltonics, Bremen, Germany)

equipped with a commercial ESI (electrospray ionization) ion source.

Synthesis of (E)-3-(4-nitrophenyl)-1-(2-(phenylsulfonylamine)phenyl)prop-2-en-1-one (3)

Compound **1** (275.1 mg, 1.0 mmol) and 4-nitrobenzaldeyde (151.1 mg, 1.0 mmol) were dissolved in 5 mL of dichloromethane, 5 mL of basic 2-propanol (62.5 mg of metallic sodium dissolved in 5 mL of 2-propanol) was added and the mixture was allowed at ambient temperature (25 °C) for 50 min. Then 30 mL of dichloromethane was added, and the solution was extracted with water until the water phase became neutral. The dichloromethane phase was dried, and the crude product was purified *via* flash columns chromatography (normal phase; 7:3 hexane/acetate and pure dichloromethane) to afford a yellow crystalline powder (125 mg, 30.6%). Mp 229–231 °C. ^{1}H NMR (CDCl$_3$) δ 7.16 (ddd, J 7.94, 7.34, 1.06 Hz, 1H), δ 7.42 (m, 2H), δ 7.48 (m, 1H), δ 7.51 (d, J 15.60 Hz, 1H), δ 7.53 (ddd, J 8.41, 7.29, 1.51 Hz, 1H), δ 7.73 (d, J 15.65 Hz, 1H), δ 7.76 (m, 3H), δ 7.87 (m, 3H), δ 8.30 (m, 2H), δ 11.22 (s, 1H); ^{13}C NMR (CDCl$_3$) δ 120.32, 123.11, 123.79, 124.32, 125.72, 127.28, 129.09, 130.79, 133.02, 135.08, 139.39, 140.29, 140.48, 142.56, 148.77, 191.97. HRMS calculated for C$_{21}$H$_{15}$N$_2$O$_5$S 407.0707, found 407.0713.

Reactivity toward GSH

Michael reaction of compounds 2, 3, 5 and 6 with GSH

To evaluate in vitro reactivity of the compounds towards GSH, 100 μL of a freshly prepared pH 3.2 aqueous solution of GSH (containing 1.875×10^{-3} and 7.5×10^{-3} mmol for study at lower and higher concentration of GSH, respectively,) were mixed with 900 μL of a freshly prepared DMSO solution containing 6.25×10^{-4} mmol of the chalcones **2**, **3**, **5** and **6**. The mixtures were incubated in a water bath at 37 °C, and the progress of the reactions was followed by HPLC with ultraviolet (UV) spectrophotometric detection. For HPLC analysis, 10 μL of the incubate diluted with 990 μL of mobile phase and immediately analyzed as described below (2.2.3.). Two parallel experiments were performed.

Retro-Michael reaction of the conjugates

In order to study the reverse (retro-Michael) reaction of the GSH conjugates to the respective chalcones, incubations were performed as described above using GSH solution of the higher (7.5×10^{-3} mmol) concentration. After the equilibrium was reached (100 min for compounds **2** and **3**, and 60 min for compounds **5** and **6**), 10 μL of the incubate was diluted with 990 μL of a mixture of methanol/water

(75:25 v/v). The obtained dilution was immediately analyzed by HPLC as described below. Analysis of the samples was repeated after 10, 20, 30, 40, 50 and 120 min standing at room temperature in the dark.

HPLC-UV/Vis measurements

HPLC analyses were performed with an Agilent 1100 (Agilent Technologies, Waldbronn, Germany) integrated system equipped with a quaternary pump, a degasser, an autosampler, and a variable wavelength UV-Vis detector. Data were recorded and evaluated by use of Agilent Chem Station (Rev. B.03.01) software.

The components were separated on a Zorbax Eclipse XDB-C8 column (150 × 4.6 mm, 5- μm particle size; Agilent Technologies, Waldbronn, Germany) at room temperature. The flow rate was 1.0 mL min^{-1}, and isocratic elution with a mobile phase of 25:75 v/v mixture of water and methanol containing 0.1 % (v/v) trifluoroacetic acid was used. The injection volume was 20 μL. Detection was performed at $\lambda = 302$, 321, 302 and 316 nm wavelength for the analysis of **2**, **3**, **5** and **6**, respectively.

HPLC–UV–ESI/MS investigations

HPLC-UV-ESI/MS analyses were performed with an Ultimate 3000 UHPLC Focused Probe (Thermo Scientific, Germering, Germany) integrated system equipped with a quaternary pump, a degasser, an autosampler and a column compartment. The components were separated on the same Zorbax Eclipse XDB-C8 column (150 × 4.6 mm, particle size 5 μm) used for the HPLC-UV/Vis assays. Chromatography was performed at 25 °C, with a flow rate of 1.0 mL min^{-1} and the injection volume of 50 μL. For the elution of the compounds, a binary gradient was mixed from mobile phases A and B (A: water 0.1% formic acid; B: methanol 0.1% formic acid) by the following profile: 50% A: 50% B for 10 min followed by a linear program to 25% A: 75% B in 10 min to keep in this last solvent composition for 5 min before returning to the initial conditions in 1 min for an additional 4 min to equilibrate the column for the next injection. UV detection was performed at 302 nm. The mass spectrometer was a Q Exactive™ Focus hybrid quadrupole-Orbitrap™ instrument (Thermo Scientific, Bremen, Germany) operated with electrospray ionization (ESI) in alternating positive and negative ion modes, as well as subsequent all-ion fragmentation to obtain tandem mass spectra (MS/MS) through collision-induced dissociation (CID) of both positive and negative ions within one cycle of acquisitions. Spray voltage and the capillary temperature of the Ion-MAX interface were held at ±4.5 kV at 300 °C, respectively. The following ESI parameters were kept constant during the analysis: sheet gas and auxiliary gas

(both N_2) flow rates of 65 and 20 units (arbitrary), respectively; desolvation temperature of 500 °C. All scans were recorded in the *m/z* 100 to 1000 (Th) range with the mass resolution set to 35,000 at m/z 400. Data were recorded and evaluated using Thermo Scientific's Xcalibur™ software (version 4.1).

Identifications were supported by accurate mass measurements performed at high mass resolution. Mass accuracies (expressed as the difference between measured and expected m/z) were <5 ppm. The chalcones gave predominantly negative ions, while the quinolone-chalcone hybrids yielded mostly positive ions. The conjugates displayed in-source fragmentation to the ionized precursor compounds and ionized GSH. The assignment of these fragment ions was confirmed by their accurate masses both from the full-scan MS and the CID-MS/MS spectra.

Crystallography

Suitable single crystals of compounds **2** and **5** were collected at room temperature using the Bruker APEX II CCD diffractometer with graphite-monochromated MoKα radiation ($\lambda = 0.71073$ Å). The structures were solved by direct methods and refined by full–matrix least squares on F^2 using SHELXL2014 software (Sheldrick 2008), available on WingX suit programs (Farrugia 2012). Compound **2** ($C_{22}H_{16}N_2O_4S$), had its structure determined from 30977 reflections collected and 3950 unique reflections, while compound **5** ($C_{28}H_{19}N_2O_5ClS$), had its structure determined from 64756 reflections collected and 6703 unique reflections. All the hydrogen atoms were placed in calculated positions and refined with fixed individual displacement parameters [$U_{iso}(H) = 1.2U_{eq}$ or $1.5U_{eq}$] according to the riding model (C–H bond lengths of 0.97 and 0.96 Å, for aromatic and methyl groups, respectively). The unit cells found measure: $a = 14.0149(16)$ Å, $b = 7.6562(9)$ Å, $c = 18.380(2)$ Å and beta $= 101.242(4)$ Å for **2** and a $= 10.2889(4)$ Å, b $= 12.3983(4)$ Å, c $= 23.8857(8)$ Å and beta $= 55.021(3)$ Å for **5**. Molecular representations and pictures were generated by Mercury (Macrae et al. 2006) and Ortep (Farrugia 2012) programs.

Theoretical calculations

The starting geometries used in the calculations were taken directly from the X-ray data and their energies (single point) were calculated by using the Density Functional Theory (DFT) as implemented in the Gaussian 09 package of programs (Frisch et al. 2009). The extended Gaussian basis set 6-311 ++ G(d,p) of Pople and co-workers (Krishnan et al. 1980; Schlegel et al. 1984) with B3LYP functional (Yanai et al. 2004) were employed throughout the calculations.

Antitumor tests

Cytotoxicity of the compounds has been tested by means of the universally used MTT method (Skehan et al. 1980). The method was first described by Mosmann (Mosmann 1983), having the ability to analyze the viability and the metabolic state of the cells. This cytotoxicity study allows one to define cytotoxicity, but not the mechanisms of anticancer action (Berridge et al. 1996). Human tumor cell lines SF-295 (glioblastoma), PC-3 (prostate) and HCT-116 (colon) were used. The cells were given by the National Cancer Institute (USA) and cultured in Roswell Park Memorial Institute (RPMI) 1640 medium, supplemented with 10% fetal bovine serum and 1% antibiotic, kept in an oven at 37 °C and 5% CO_2 atmosphere. The samples were diluted in pure sterile dimethyl sulfoxide (DMSO) and were tested in a single concentration of 25 µg mL^{-1}. Statistical analysis of the experiments was performed according to the mean and standard error of the mean (SEM) of the percentage of cell growth inhibition, using the GraphPad Prism 7.00 program (GraphPad).

Compounds which had a percentage of inhibition of tumor growth greater than 75% in at least one tumor line tested were tested again by serial dilution (dilution factor = 2), starting from the highest 25 µg mL^{-1} concentration for determination of concentration capable of inhibiting 50% of cell proliferation (IC_{50}). The experiments were analyzed by a non-linear regression curve for the calculation of IC_{50} using the GraphPad Prism program. Doxorubicin was used as a positive control.

Results and discussion

Synthesis

2'*N*-phenylsulfonylacetophenone (**1**) was obtained from the reaction of benzenesulfonyl chloride and 2-aminoacetophenone in dichloromethane as previously described (de Castro et al. 2016; de Castro et al. 2017; d'Oliveira et al. 2018). Compounds **2** and **3** and **4** were synthesized by base-catalyzed Claisen-Schmidt condensation between **1** and the respective substituted benzaldehyde (Scheme 1). Structure of compounds **2** and **4** were verified by their ^{1}H NMR spectra.
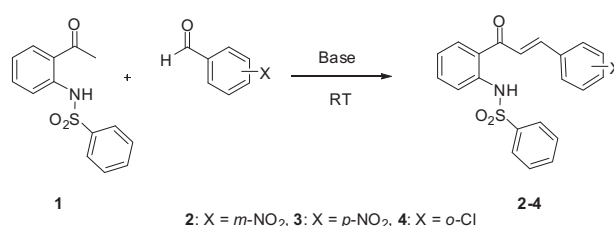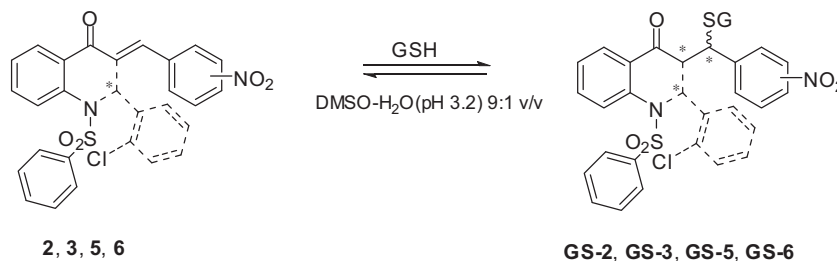

Scheme 1 General conditions for the synthesis of chalcones **2–4**

Scheme 2 Synthesis of chalcone–quinolinone compounds **5** and **6**

5: X = *m*-NO$_2$, **6**: X = *p*-NO$_2$
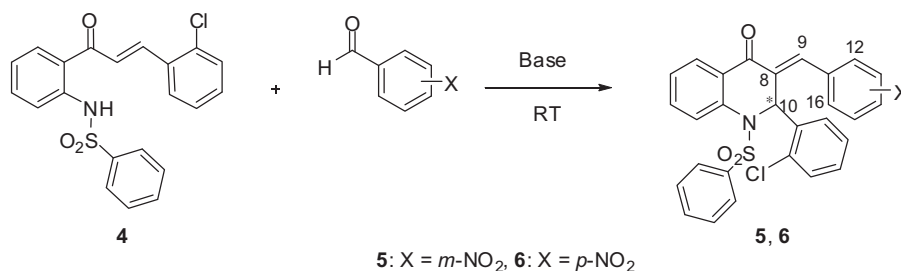
Scheme 3 Conjugation reaction of compounds **2**, **3**, **5** and **6** with GSH

^{1}H NMR spectra of the newly synthetized **3** show direct evidence of the desired reaction. The two doublets of $\delta = 7.32$ ppm and $\delta = 8.03$ ppm with the coupling constant of $J = 15.6$ Hz, demonstrate the presence of an *(E)* α, β-unsaturated carbonyl moiety. On the other hand, the singlet observed at $\delta = 11.3$ ppm for both compounds - a chemical shift typical for the sulfonamide hydrogens - corroborate the aminosulfonyl linkage. Intramolecular hydrogen bonding between the carbonyl and the NH groups, forming a six-membered ring, justifies this relatively high chemical shift of the proton.

Compounds **5** and **6** were obtained by reacting compound **4** with *m*-nitrobenzaldehyde and *p*-nitrobenzaldehyde under basic condition (Scheme 2). Their structure was verified by their ^{1}H NMR spectra (d'Oliverira et al. 2018).

Reactivity toward GSH

In these reactions, the nucleophilic sulfur atom of GSH is added to the β-carbon, followed by proton transfer reaction to the α-carbon generating new chiral centers. GSH-adducts of the open-chain chalcones (**2** and **3**) have one, quinolone-chalcones (**5** and **6**) have three newly formed stereogenic centers in addition to the two inherent (enantiomerically fixed) stereocenters of GSH (Scheme 3). Accordingly, in the case of **2** and **3** formation of two, in the case of **5** and **6** formation of eight diastereomeric adducts can be expected (Perjési et al. 2012; Bernardes et al. 2017; Bernardes et al. 2018).

The HPLC-UV chromatograms of the incubates showed three peaks for compounds **2** and **3**, and five peaks for compounds **5** and **6**, attributed to the expected isomeric adducts and the starting chalcones with the following

retention times: **GS-2 a1**: 10.3, **GS-2 a2**: 10.6, **2**: 20.0; **GS-3 a1**: 11.0, **GS-3 a1**: 11.2, **3**: 19.7; **GS-5 a1**: 16.1, **GS-5 a2**: 16.3, **GS-5 b1**: 17.7, **GS-5 b2**: 17.9, **5**: 22.2; **GS-6 a1**: 17.4, **GS-6 a2**: 17.6, **GS-6 b1**: 18.5, **GS-6 b2**: 18.6, **6**: 22.8. Figures 2 and 3 illustrate the analyses of compounds **2** and **5**, respectively.

The occurrence of the conjugation reactions was confirmed by LC-ESI-MS analysis for each peak observed in the chromatograms. Figures 2 and 3 illustrate the results for compounds **2** and **5**, respectively. Besides the deprotonated and protonated molecules of each precursor ([M-H]$^-$ for compounds **2** and **3**, [M + H]$^+$ for compounds **5** and **6**), ESI-MS analysis of each incubation confirmed the presence of the respective GSH conjugates. These latter showed the following ions attributed to the respective deprotonated and protonated molecules: **GS-2 a1** and **a2** at *m/z* 714 [M−H]$^-$, **GS-3 a1** and **a2** *m/z* 714 [M−H]$^-$, **GS-5 a1**, **a2**, **b1** and **b2** at m/z 838 [MH]$^+$ and **GS-6 a1**, **a2**, **b1** and **b2** at *m/z* 838 [MH]$^+$ (accurate masses and mass errors relative to expected *m/z* values calculated from elemental compositions are given in Figs. 2 and 3). GSH conjugates also displayed characteristic ion fragmentation in the ESI source of the instrument, while the chalcones (**2**, **3**) and the quinolinone-chalcone hybrids (**5**, **6**) required CID to produce structure-related fragment ions for MS/MS analysis. The respective mass spectra of compounds **3** and **6** can be found in Figure S19 and Figure S20 of the Supplementary Data.

It is worth noting that in the chromatograms of the incubates of **5** and **6** only two pairs of peaks were observed, which might correspond to two pairs of diastereomeric adducts. Such a reduction in the number of the formed diastereomers can be explained by the selective formation
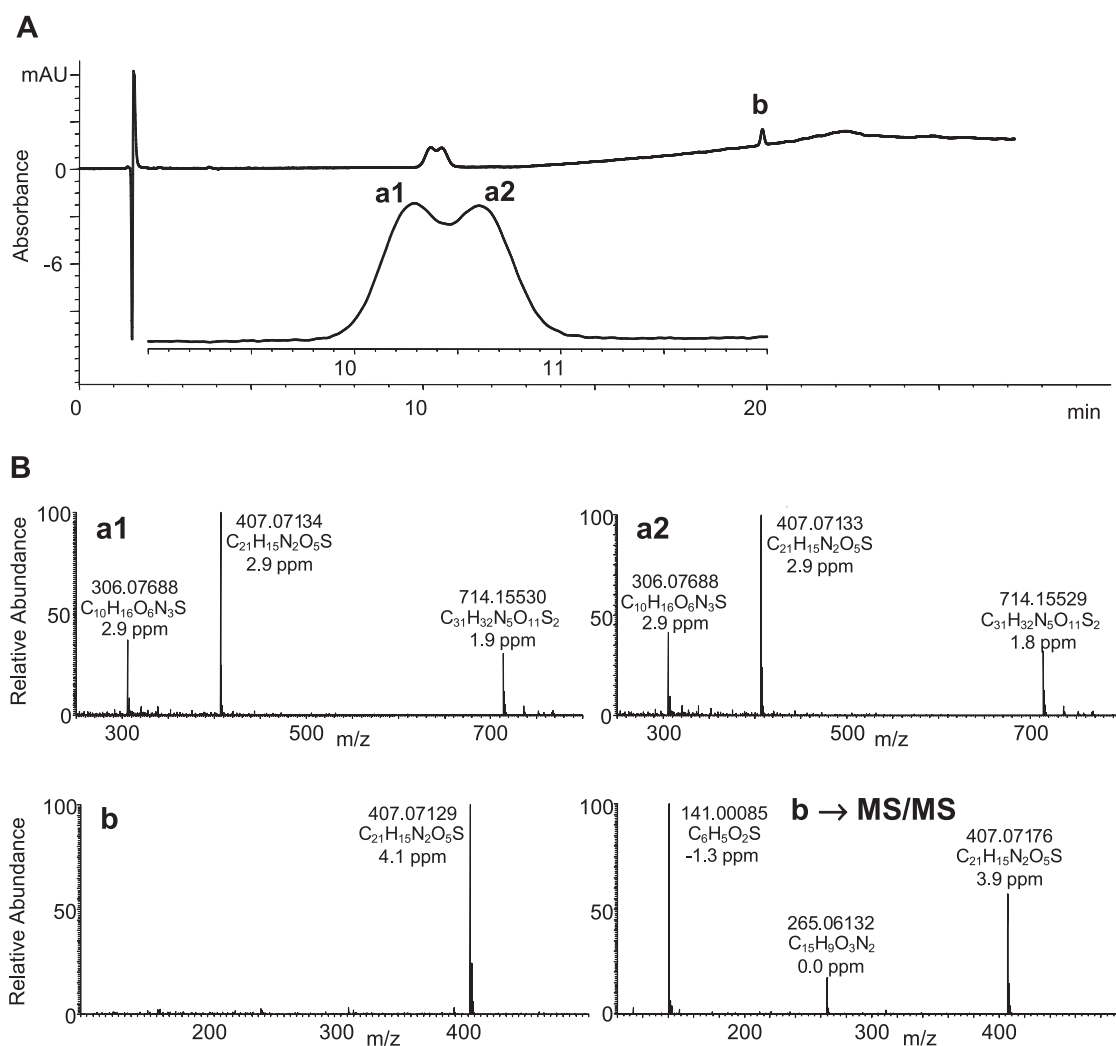
Fig. 2 **a** HPLC analysis of the mixture of **2** and their GSH conjugates, along with (**b**) negative-ion ESI mass spectra of **a1** and **a2** diastereomers of the **GS-2** conjugates and negative-ion ESI mass spectra and
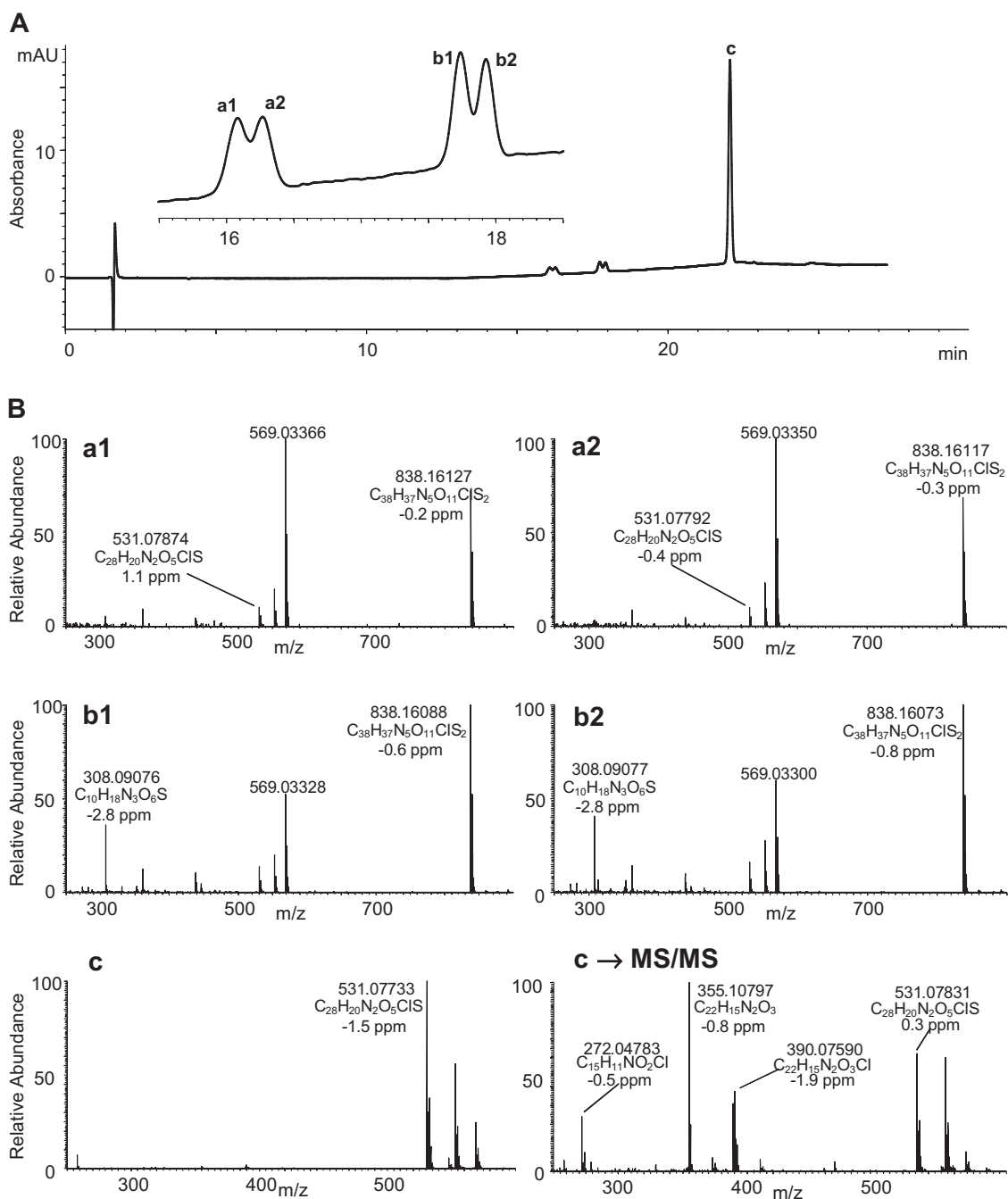
MS/MS of **2** (**b**) obtained by LC-ESI-MS analyses. Assays were performed with the 10-min incubation sample of compound **2** using 7.5 mmol L^{-1} initial GSH concentration

of the *trans* diastereomers because of the conformationally restricted orientation of the bulk C10-aryl group (see Scheme 2). Thiol addition onto the oxygen-counterpart 2-phenyl-(E)-3-benzylidene-chroman-4-ones also resulted in the formation of the corresponding *trans* adducts with respect to the C8-C10 H-atoms (Osama et al. 2014) However, determination of the exact stereochemistry of the formed adducts needs further synthetic and analytical experiments.

The employed HPLC-UV conditions of analysis of the incubates allowed to determine the amount of the remaining chalcones as a function of the incubation time. Figure 4 shows typical chromatograms of these incubations. The retention times of compounds **2**, **3**, **5** and **6** are 3.3, 3.2, 4.3 and 5.0 min, respectively. Although close to the dead volume, it was also possible to detect the diastereomeric peaks of the GSH conjugates.

Figures 5 and 6 show the concentration of the remaining chalcones as a function of incubation times at a higher (upper graph) and a lower (lower graph) GSH concentration. In the equilibrium mixtures of the higher (7.5 mmol L^{-1}) and the lower (1.875 mmol L^{-1}) GSH concentration, the amount of the unreacted chalcone **2** and **3** was near 3 and 10% of the initial value, respectively. On the other hand, much higher amount of unreacted quinolinone-chalcones could be detected in the equilibrium mixtures of compounds **5** and **6** (reacting under the same conditions): compound **5**: 72% (higher concentration of GSH) and 92% (lower concentration of GSH); compound **6**: 77% (higher concentration of GSH) and 93% (lower concentration of GSH).

The results indicate that all four compounds reach the equilibrium conditions in a relatively short time. The amounts of the formed GSH-conjugates at equilibrium are much higher in the case of the sulfonamide chalcones (**2** and

Fig. 3 a HPLC analysis of the mixture of 5 and their GSH conjugates, along with (b) positive-ion ESI mass spectra of a1, a2, b1 and b2 diastereomers of the GS-5 conjugates and positive-ion ESI mass spectra and MS/MS of 5 (c) obtained by LC-ESI-MS analyses. Assays were performed with the 10-min incubation sample of compound 5 using 7.5 mmol L^{-1} initial GSH concentration

3) than for the cyclic quinolinone-chalcones (5 and 6). The initial GSH:chalcone ratio has limited influence on the composition of the equilibriums. Accordingly, the equilibrium is thermodynamically controlled, and the time needed to reach the equilibrium is determined by the rates of the forward and the backward reactions.

As a model, the kinetic rate law for second- and first-order reversible reactions (Lavabre et al. 1993) was considered:
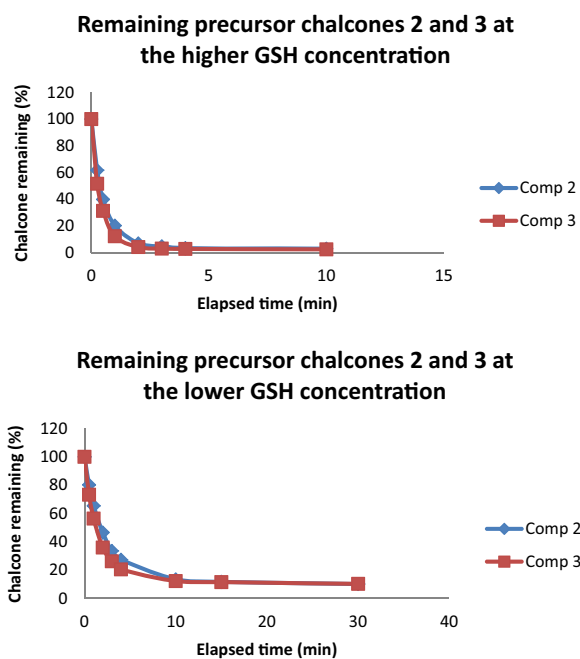
$$A + B \rightleftharpoons C \quad v = k_1[A][B] - k_2[C] \tag{1}$$

The velocity (v) in Eq. (1) of the cited publication is a function of k_1 (forward reaction), k_2 (reverse reaction) and t (time). Using data from 0 to 4 min from the reactions with the higher (7.5 mmol L^{-1}) GSH concentration, k_1 and k_2 were obtained through curve fitting and given in Table 1.
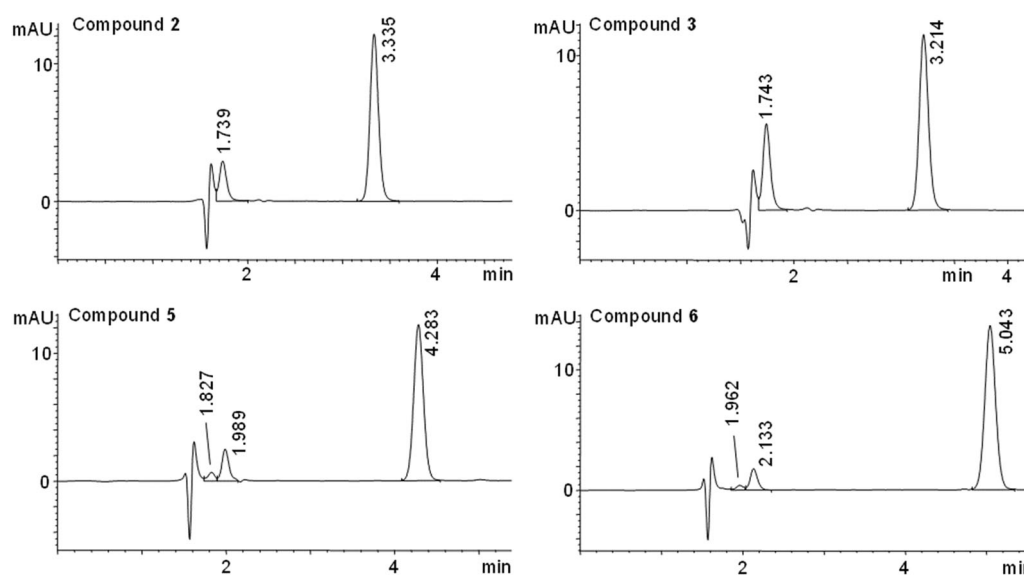
Fig. 4 Typical HPLC-UV chromatograms of incubations of compounds **2**, **3**, **5** and **6**

Fig. 5 Remaining percentage chalcone *versus* time of incubation for compounds **2** and **3**: Reactions in DMSO:H$_2$O (9:1 v/v) at higher (7.5 mmol L^{-1}) and lower (1.875 mmol L^{-1}) GSH concentration
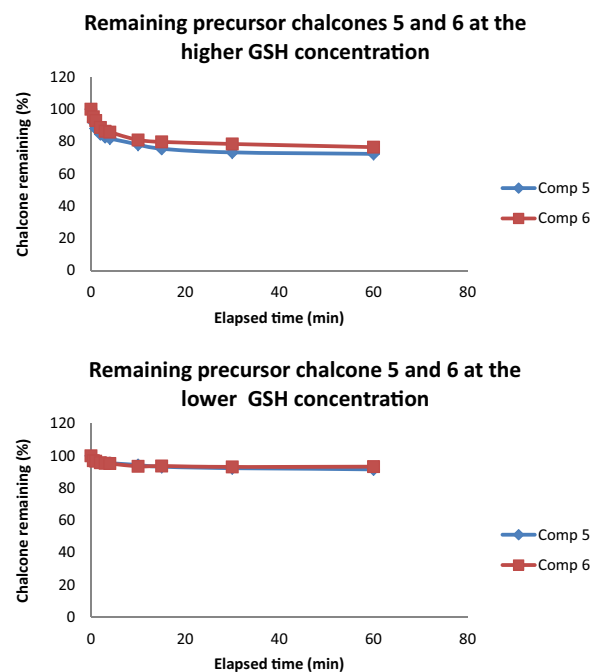
Fig. 6 Remaining percentage chalcone *versus* time of incubation for compounds **5** and **6**: Reactions in DMSO:H$_2$O (9:1 v/v) at higher (7.5 mmol L^{-1}) and lower (1.875 mmol L^{-1}) GSH concentration

The difference between the values of k_1 for the compounds **2** and **3** may be rationalized by the strong electron withdrawing effect of the *para*-nitro group, which decreases the electron density of the β-carbon, making the nucleophilic attack of the GSH thiol group easier. On the contrary, a different pattern has been observed on comparison of the k_1 values of compounds **5** and **6**. In this case, it can be supposed that, due to the non-planar structure of the enone moiety, transmission of the *para*-nitro group's effect is not

Table 1 Calculated k_1 and k_2 using the kinetic model of equilibria (1)

| Compound	2	3	5	6
k_1	127.5	171.4	26.1	13.4
k_2	0.025	0.034	0.880	0.536

so effective, and the inductive effect of the *meta*-nitro group reduces the electron density of the β-carbon atom more

profoundly. Comparison of the differences of the k_1 values of compounds **2** and **3** to those of **5** and **6** can justify the difference in the times needed to reach the equilibrium of the two sets of chalcone derivatives.

These findings allowed us to make two conclusions. First, it is possible to change the structure of the highly thiol-reactive chalcones (**2** and **3**) and convert the molecules into moderately (5–15-times) less reactive derivatives such as the quinolinones **5** and **6**. Second, as a consequence of the somewhat reduced thiol-reactivity and, moreover, more profoundly (15–35-times) reduced stability of the resultant GSH adducts, derivatives (**5** and **6**) may not reduce cellular GSH as much as the corresponding open-chain chalcones (**2** and **3**). According to the conclusions drawn from earlier studies (Dinkova-Kostova et al. 2001; Jin et al. 2008) the quinolinone-chalcone hybrids (**5** and **6**) would be expected therefore to show lower antitumor effect than that of the open-chain chalcones (**2** and **3**).

The above reactions were performed in a basically polar non-protic medium (DMSO with 10% H_2O) due to the poor solubility of the chalcones in polar protic solvents. To investigate how the reverse reaction might proceed in a protic medium (mimicking physiological conditions), the reverse reaction was studied in a methanol/water (75:25 v/v) mixture. Figure 7 shows the amount of the remaining GSH-adduct as a function of time, indirectly determined by measuring the amount of the respective precursor chalcone (**2**, **3**, **5** and **6**).

As the results shown in Fig. 7 demonstrate, the rate of decomposition (retro-Michael reaction) of the open-chain chalcone-GSH conjugates (**GS-2** and **GS-3**) is very slow confirming the results presented in Table 1. On the contrary, the rate of the reverse reaction of the cyclic quinolinone-chalcone-GSH adducts (**GS-5** and **GS-6**) is much faster. Similar results were obtained in the experiments performed in the DMSO-H_2O (90:10 v/v) mixture.
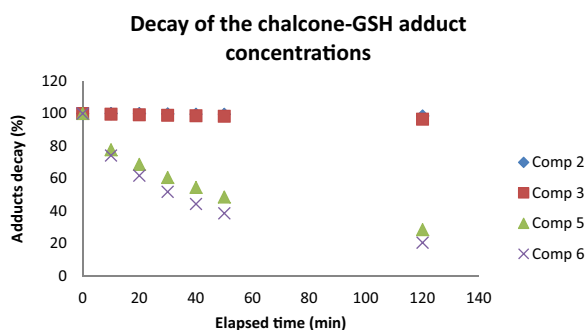
Fig. 7 Decay of the GSH-adduct of chalcones **2**, **3**, **5** and **6** (**GS-2**, **GS-3**, **GS-5** and **GS-6**, respectively) in a methanol/water (75:25 v/v) mixture

Structural and theoretical analysis

To provide explanations on how the molecular structure could affect this non-enzyme catalyzed nucleophilic addition, crystal structures of compounds **2** and **5** were obtained from single crystal X-ray diffraction. Both **2** and **5** have crystallized under monoclinic centrosymmetric space group P 2_1/c. The crystallographic refinement of **2** led to a model with $R_1 = 5.27\%$ and $Goof = 1.045$ and the model proposed for **5** has $R_1 = 6.21\%$ and $Goof = 1.054$. An Ortep representation (Farrugia 2012) showing the thermic atomic displacements of both compounds is given in Fig. 8.

As it is shown in Fig. 9, some characteristic differences can be noted between the crystal structures of compounds **2** (represented by blue color) and **5** (represented by cyan color) as a result of the cyclization reaction. It was found that the sulfonyl group adopts a -*syn*-periplanar conformation regarding the carbonyl group (∟N2-C15-C9-O1 = −3.72°) in compound **2**, while a +*anti*-periplanar one (∟N2-C10-C12-O1 = 168.07°) in compound **5**. This different conformation of compound **5** is the result of rotation of the aromatic ring of the benzylidene moiety and contributes to a steric hindrance of the *β*-carbon atom (the GSH reaction site). The presence of the chlorophenyl group in compound **5** also contributes to steric hindrance, which corroborates explanation its lower k_1 in comparison to compound **2** (see Table 1).

The planarity of **2** and **5** can be evaluated from the chalcone backbone. In **2**, this moiety can be considered planar, since the nitro group has a torsion close to 180° regarding the olefin portion (+*anti*-periplanar conformation, with ∟C8-C7-C2-N1 = 176.51°). In contrast, deviation from planarity of the chalcone moiety of **5** is confirmed by analyzing this same dihedral angle, which is for a -*syn*-clinal conformation (∟C8-C7-C2-N1 = −36.80°). Because of this planarity deviation, **2** is more stabilized by conjugation than **5**. In addition, since the GSH-reaction is a nucleophilic addition, positive charges close to the *β*-carbon contributes to k_1. Accordingly, the higher k_1 for compound **2** is also explained by the presence of the *α*-proton (to the carbonyl group), which is missing in compound **5**.

Theoretical calculations also were performed to explain the trend of k_1 values from Table 1. In Fig. 10, the shape and the energies of the highest occupied molecular orbital (HOMO) and the lowest unoccupied molecular orbital (LUMO) of the studied compounds are shown. The HOMO indicates the regions where the molecule acts as an electron donor, while LUMO indicates the acceptor regions. For **2**, the LUMO is close only to the chalcone backbone and has the energy of $E_{LUMO} = −3.19\,eV$, and the HOMO is concentrated on both the benzenesulphonyl group and the ring nitrogen with the energy of $E_{HOMO} = −6.88\,eV$. Similar to **2**, the LUMO of compound **5** is also over the chalcone
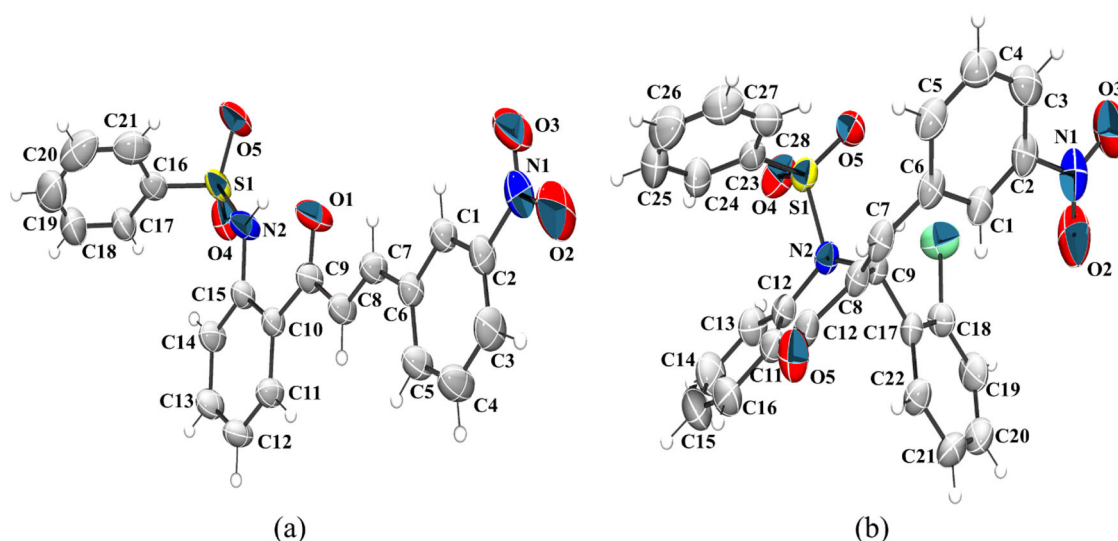
Fig. 8 Ortep representation showing the thermal displacement of **2** (**a**) and **5** (**b**) with 50% probability. Hydrogens displayed as spheres with arbitrary radii
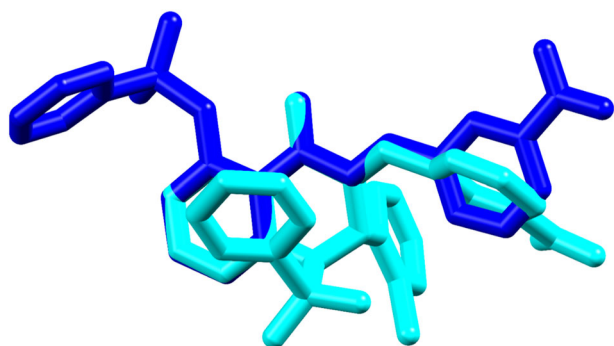
Fig. 9 Overlapping of crystal structures of **2** (represented by blue color) and **5** (represented by cyan color) showing the main differences between them. The aromatic ring closer to carbonyl group was used as a fixed point

backbone, but with higher energy ($E_{LUMO} = -2.96\,eV$), while the HOMO is mostly spread over the chlorobenzene group ($E_{HOMO} = -6.93\,eV$). This difference of HOMO and LUMO energies implies a lower gap energy for compound **2** ($E_{GAP} = 3.69\,eV$), indicating a higher reaction susceptibility.

Molecular electrostatic potential surfaces of **2** and **5** are presented in Fig. 11. This surface is an electron density map that also indicates the donor regions (represented by blue color) and the acceptor regions (represented by red color). Lower energies are found over the sulfonyl and the nitro group ($\delta^- \approx -1.47\,eV$ for **2** and $\delta^- \approx 1.42\,eV$ for **5**), while higher energies are concentrated close to the olefin portion and the β-carbon ($\delta^+ \approx 1.33\,eV$ for **2** and $\delta^+ \approx 0.61\,eV$ for **5**). In addition, theoretical calculations indicated a positive partial charge on the β-carbon of compound **2** ($\delta^+ = 3.92\,eV$), which contributes to the GSH addition reaction, and negative partial charge on β-carbon from compound **5**

($\delta^- = 5.89\,eV$), which contributes to GSH elimination reaction.

Antitumor potency

Cytotoxicity of the compounds has been tested by means of the universally used MTT method (Skehan et al. 1980). The results of the cytotoxicity testing of compounds **2**, **3**, **5** and **6** against PC-3 (prostate), HCT-116 (colon) and SF-295 (glioblastoma) human tumor cell lines are shown in Table 2.

Among the tested compounds, **2**, **3** and **6** were considered to be cytotoxic with a percentage of inhibition of tumor growth in some cell line greater than 75% (taking in account the standard deviations). Table 3 presents the IC_{50} values of the tested compounds.

As it is shown, it was not possible to find an unambiguous correlation in the ring substitution of **2** to **3** or **5** to **6**, and their antitumor activity. Specifically, compound **2** (*meta*-substituted) showed higher potency towards PC3 and HTC-116, and lower to SF-295, comparing it with compound **3** (*para*-substituted). In turn, compound **5** (*meta*-substituted) showed higher potency to inhibit tumor growth of SF-295 cells, and lower one of the PC3 and HTC-116 cells in comparison with compound **6** (*para*-substituted). The average inhibition of the chalcones **2** and **3** was 60%, while the average inhibition of the chalcone-quinolinones **5** and **6** was 62%. Therefore, although GSH-reactivity of compounds **5** and **6** was considerably lower than that of **2** and **3** (as shown in Table 1), the average inhibition of tumor growth of the compounds was similar.

The results suggest that conjugation with GSH or with other SH-reactive cellular thiols is not a determining factor in the antitumor activities of the compounds. This is in
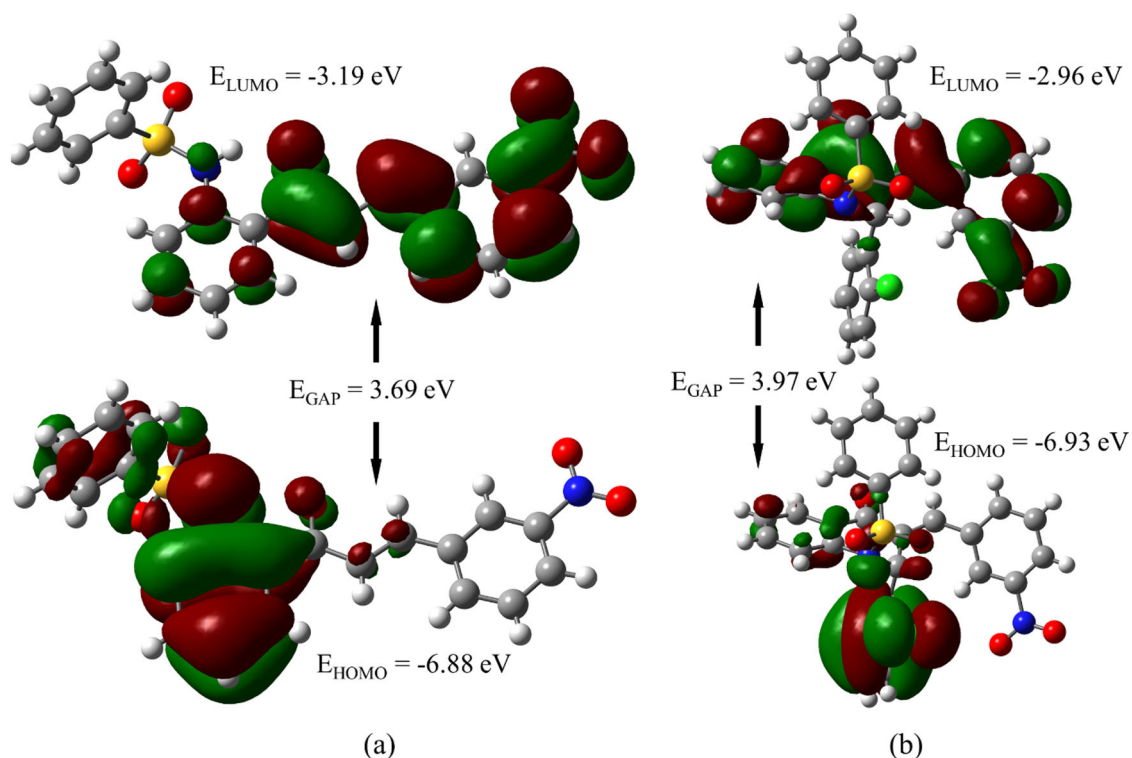
Fig. 10 Frontier molecular orbitals of compounds **2** (**a**) and **5** (**b**). Energies (E) of the highest occupied molecular orbital (HOMO) and lowest unoccupied molecular orbital (LUMO) are shown. E_{GAP} is the difference between E_{LUMO} and E_{HOMO}
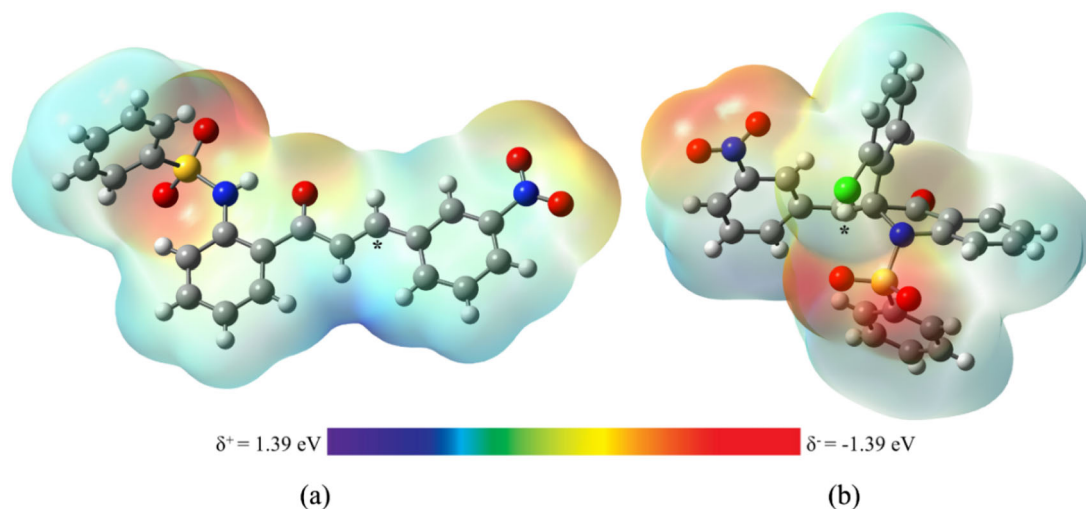
Fig. 11 Molecular electrostatic potential (MEP) of compounds **2** (**a**) and **5** (**b**). In both representations the β-carbon is marked. Red regions indicate high electron density and blue regions indicate low electron density

agreement with the results of our previous studies with cyclic chalcone analogues. It was found that the derivatives with the highest antitumor activities are those ones with substituents with strong electron-donating character on the benzylidene moiety (Dimmock et al. 1999). Cell cycle analysis of Jurkat-

T cells exposed to the compounds showed a characteristic G2-M block suggesting their microtubule activity (Rozmer et al. 2006). Chalcone-tubulin interaction has been demonstrated in several previous publications (Stanton et al. 2011; Martel-Frachet et al. 2015; Lindamulage et al. 2017).

Table 2 Percentage inhibition of tumor growth by compounds **2**, **3**, **5** and **6** in vitro compared to untreated control at a single concentration of 25 μg mL^{-1} in three human tumor cell lines (PC3, HTC-116 and SF-295) after 72 h of treatment as determined by the MTT method

Compound	PC3	HTC-116	SF-295
2	77.9 ± 3.4	66.8 ± 0.9[a]	63.5 ± 1.1
3	45.0 ± 0.2	25.7 ± 1.4	81.5 ± 2.5
5	49.6 ± 1.2	72.8 ± 0.5[a]	60.1 ± 1.6
6	68.4 ± 0.3	73.4 ± 2.4[a]	50.1 ± 2.1

[a]From d'Oliveira et al. (2018)

Table 3 IC$_{50}$ (μg mL^{-1}) values (with 95% confidence intervals in parentheses) for compounds **2**, **3** and **6** in tumor cell lines after 72 h of treatment, as determined by the MTT method

Entry	PC3	HTC-116	SF-295
2	7.9 (6.5–9.7)	6.6 (5.7–7.5)	6.9 (6.3–7.7)
3	>25	>25	11,5 (9.6–13.8)
6	>25	19.3 (13.7–27.2)[a]	>25
Doxorubicin	0.44 (0.34–0.54)	0.12 (0.09–0.17)	0.24 (0.2–0.27)

[a]From d'Oliveira et al. (2018)

Conclusion

It was shown that it is possible to substantially change equilibrium composition of the reaction of the same chalcone moiety with GSH by making a structural hybrid with a quinolinone moiety. This structural modification not only reduced thiol reactivity, but also decreased chemical stability of the formed GSH-adducts of the compounds. On the other hand, these structural differences did not influence the biological activity of the compounds; antitumor potencies remained unchanged despite the very different equilibrium compositions of the chalcone-GSH incubates under the investigated conditions. Overall, the present results support a non-thiol reactivity-based biological action of the investigated chalcone derivatives.

Compliance with ethical standards

Conflict of interest The authors declare that they have no conflict of interest.

Publisher's note: Springer Nature remains neutral with regard to jurisdictional claims in published maps and institutional affiliations.

References

Amslinger S (2010) The tunable functionality of α,β-unsaturated carbonyl compounds enable their differential application in biological systems. ChemMedChem 5:351–356

Bansal A, Simon MC (2018) Glutathione metabolism in cancer progression and treatment resistance. J Cell Biol. 217:2291–2298

Bernardes A, d'Oliveira GDC, Silezin A, Kuzma M, Molnár S, Pérez CN, Perjési P (2018) Reagent-induced asymmetric induction in addition reaction of reduced glutathione onto bis-Mannich chalcones. Arch Pharm 351:1700386. https://doi.org/10.1002/ardp.201700386

Bernardes A, Pérez CN, Mayer M, Da Silva CC, Martins FT, Perjési P (2017) Study of reactions of two Mannich bases derived of 4′-hydroxychalcones with glutathione by RP-TLC, RP-HPLC and RP-HPLC-ESI-MS analysis. J Braz Chem Soc 28:1048–1062

Berridge MV, Tan AS, McCoy KD, Wang R (1996) The biochemical and cellular basis of cell proliferation assays that use tetrazolium salts. Biochemica 4:14–19.

de Castro MRC, Aragão AQ, da Silva CC, Pérez CN, Queiroz DPK, Queiroz Jr LHK, Barreto S, de Moraes MO, Martins FT (2016) Conformational variability in sulfonamide chalcone hybrids: crystal structure and cytotoxicity. J Braz Chem Soc 27:884–898

de Castro MRC, Naves RF, Bernardes A, da Silva CC, Pérez CN, Moura AF, de Moraes MO, Martins FT (2017) Tandem chalcone-sulfonamide hybridization, cyclization and further Claisen-Schmidt condensation: Tuning molecular diversity through reaction time and order and catalyst. Arab J Chem. https://doi.org/10.1016/j.arabjc.2017.11.005

Dimmock JR, Kandepu NM, Nazarali AJ, Kowalchuk TP, Motaganahalli N, Quail JW, Mykytiuk P, Audette GF, Prasad L, Perjési P, Allen TM, Santos CL, Szydlowski J, De Clercq E, Balzarini J (1999) Conformational and quantitative structure-activity relationship study of cytotoxic 2-arylidenebenzocycloalkanones. J Med Chem 42:1358–1366

Dinkova-Kostova AT, Massiah MA, Bozak RE, Hicks RJ, Talalay P (2001) Potency of Michael reaction acceptors as inducers of enzymes that protect against carcinogenesis depends on their reactivity with sulfhydryl groups. Proc Natl Acad Sci USA 98:3404–3409

d'Oliverira GDC, Moura AF, de Moraes MO, Pérez CN, Liao LM (2018) Synthesis, characterization and evaluation of in vivo antitumor activities of novel chalcone-quinolinone hybrid compounds. J Braz Chem Soc 29:2308–2325

Estrela JM, Ortega A, Obrador E (2006) Glutathione in cancer biology and therapy. Crit Rev Clin Labor Sci. 43:143–181

Farrugia LJ (2012) WinGX and ORTEP for Windows: an update. J Appl Crystallogr. 45:849–854

Frisch MJ, Trucks GW, Schlegel HB, Scuseria GE, Robb MA, Cheeseman JR, Scalmani G, Barone V, Mennucci B, Petersson GA, Nakatsuji H, Caricato M, Li X, Hratchian HP, Izmaylov AF, Bloino Zheng JG, Sonnenberg JL, Hada M, Ehara M, Toyota K, Fukuda R, Hasegawa J, Ishida M, Nakajima T, Honda Y, Kitao

O, Nakai H, Vreven T, Montgomery Jr JA, Peralta JE, Ogliaro F, Bearpark M, Heyd JJ, Brothers E, Kudin KN, Staroverov VN, Kobayashi R, Normand J, Raghavachari K, Rendell A, Burant JC, Iyengar SS, Tomasi J, Cossi M, Rega N, Millam JM, Klene M, Knox JE, Cross JB, Bakken V, Adamo C, Jaramillo J, Gomperts R, Stratmann RE, Yazyev O, Austin AJ, Cammi R, Pomelli C, Ochterski JW, Martin RL, Morokuma K, Zakrzewski VG, Voth GA, Salvador P, Dannenberg JJ, Dapprich S, Daniels AD, Farkas Ö, Foresman JB, J. Ortiz V, Cioslowski J, Fox DJ (2009) Gaussian 09, Revision A.02. Gaussian Inc, Wallingford CT

Go ML, Wu X, Liu XL (2005) Chalcones: an update on cytotoxic and chemoprotective properties. Curr Med Chem 12:481–499

Gomes MN, Muratov EN, Pereira M, Peixoto JC, Rosseto LP, Cravo PVL, Andrade CH, Neves BJ (2017) Chalcone derivatives: promising starting points for drug design. Molecules 2017 22:1210

GraphPad Prism version 7.00 for Windows, GraphPad Software, La Jolla, California, USA, www.graphpad.com

Harborne JB, Williams CA (2000) Advances in flavonoid research since 1992. Phytochemistry 55:481–504

Harris IS, Treloar AE, Inoue S, Sasaki M, Gorrini C, Lee KC, Yung KY, Brenner D, Knobbe-Thomsen CB, Cox MA, Elia A, Berger T, Cescon DW, Adeoye A, Brustle A, Molyneux SD, Mason JM, Li WY, Yamamoto K, Wakeham A, Berman HK, Khokha R, Done SJ, Terrance J, Kavanagh TJ, Lam CW, Mak TW(2015) Glutathione and thioredoxin antioxidant pathways synergize to drive cancer initiation and progression Cancer Cell 27:211–222

Jin YL, Jin XY, Jin F, Sohn DH, Kim HS (2008) Structure activity relationship studies of anti-inflammatory TMMC derivatives: 4-Dimethylamino group on the B ring responsible for lowering the potency. Arch Pharm Res 31:1145–1152

Krishnan R, Binkley JS, Seeger R, Pople JA (1980) Self-consistent molecular orbital methods. XX. A basis set for correlated wavefunctions. J Chem Phys 72:650–654

Lavabre JCMD, Pimienta V, Levy G (1993) Reversible, mixed first- and second-order and autocatalytic reactions as particular cases of a single kinetic rate law. J Phys Chem 97:5321–5326

Lindamulage IK, Vu H-Y, Karthikeyan C, Knockleby J, Lee Y-F, Trivedi P, Lee H (2017) Novel quinolone chalcones targeting colchicine-binding pocket kill multidrug-resistant cancer cells by inhibiting tubulin activity and MRP1 function. Sci. Reports 7:10298.

Macrae CF, Edgington PR, McCabe P, Pidcock E, Shields GP, Taylor R, Towler M, van de Streek J (2006) Mercury: visualization and analysis of crystal structures. J Appl Crystallogr 39:453–457

Martel-Frachet V, Keramidas M, Nurisso A, DeBonis S, Rome C, Coll J-L, Boumendjel A, Skoufias DA, Ronot X (2015) IPP51, a chalcone acting as a microtubule inhibitor with in vivo antitumor activity against bladder carcinoma. Oncotarget 6:14669–14686

Maydt D, De Spirt S, Muschelknautz C, Stahl W, Müller TJJ (2013) Chemical reactivity and biological activity of chalcones and other α,β-unsaturated carbonyl compounds. Xenobiotica 43:711–718

Mosmann T (1983) Rapid colorimetric assay for cellular growth and survival: application to proliferation and cytotoxicity assays. J Immunol Meth 65:55–63

Nowakowska Z (2007) A review of anti-infective and anti-inflammatory chalcones. Eur J Med Chem 42:125–137

Ortega AL, Mena S, Estrela JM (2011) Glutathione in cancer cell death. Cancers 3:1285–1310

Osama M, Hussain W, Hussain HT (2014) Two novel four fused ring system benzo-pyrano–triazolo-thiadiazepines from 2-phenyl-E-3-benzylidenechroman-4-ones: Synthesis, stereostructure and cytotoxic activity. Int J Modern Org Chem 3:18–33

Perjési P, Maász G, Reisch R, Benko A (2012) E)-2-Benzylidene-benzocyclanones: Part VII. Investigation of the conjugation reaction of two cytotoxic cyclic chalcone analogues with glutathione: An HPLC-MS study. Monatsh Chem 143:1107–1114

Perjési P, Perez CN, Bernardes A, d'Oliveira GD, Kenari F (2019) The chemistry of GST-catalyzed reactions. In: Perjési P (ed) Glutathione: biosynthesis, functions and biological implications. Nova Science Publishers, New York, NY, p 373–409

Powis G, Gasdaska JR, Baker A (1997) Redox signaling and the control of cell growth and death. In: Sies H (ed) Advances in pharmacology Vol 38. Academic Press, San Diego, p 329–359

Rahman MA (2011) Chalcone: a valuable insight into the recent advances and potential. Chem Sci J 29:1–16

Rozmer Z, Perjési P (2016) Naturally occurring chalcones and their biological activities. Phytochem Rev 15:87–120

Rozmer Z, Berki T, Perjési P (2006) Different cell proliferation effects of two cyclic chalcone analogues in Jurkat lymphocytes. Toxicol in Vitro 20:1354–1362

Sahu NK, Balbhadra SS, Choudhary J, Kohli DV (2012) Exploring pharmacological significance of chalcone scaffold: A review. Curr Med Chem 19:209–225

Schlegel HB, Binkley JS, J. Pople A (1984) First and second derivatives of two electron integrals over Cartesian Gaussians using Rys polynomials. J Chem Phys 80:1976

Sheldrick GM (2008) A short history of SHELX. Acta Crystallogr Sect A Found Crystallogr 64:112–122

Sing P, Anand A, Kumar V (2014) Recent developments in biological activities of chalcones: a mini review. Eur J Med Chem 85:758–777

Skehan P, Storeng R, Scudiero D, Monks A, McMahon J, Vistica D, Warren J, Bokesch H, Kenney S, Boyd M (1980) New colorimetric cytotoxicity assay for anti-cancer drug screening. J Natl Cancer Inst 82:1107–1112

Stanton R, Gernert KM, Nettles JH, Aneja R (2011) Drugs that target dynamic microtubules: a new molecular perspective. Med Res Rev 31:443–481

Traverso N, Ricciarelli R, Nitti M, Marengo B, Furfaro AL, Pronzato MA, Marinari UM, Domenicotti C (2013) Role of glutathione in cancer progression and chemoresistance. Oxid Med Cell Longev 2013:972913

Vaskóvá J (2019) Diverse effects of glutathione in the pathophysiology of some organ diseases. In: Perjési P (ed) Glutathione: biosynthesis, functions and biological implications. Nova Science Publishers, New York, NY, p 169–188

Wang J, Wang S, Song D, Zhao D, Sha Y, Jiang Y, Jing Y, Cheng M (2009) Chalcone derivatives inhibit glutathione S-transferase P1-1 activity: Insights into the interaction mode of a,b-unsaturated carbonyl compounds. Chem Biol Drug Res 73:511–514

Yanai T, Tew DP, Handy NC (2004) A new hybrid exchange–correlation functional using the Coulomb-attenuating method (CAM-B3LYP). Chem Phys Lett 393:51–57

Zhuang C, Zhang W, Sheng C, Zhang W, Xing C, Miao Z (2017) Chalcone: a privileged structure in medicinal chemistry. Chem. Rev 117:7762–7810